NOTICE CONCERNING COPYRIGHT RESTRICTIONS

3D Geological Mapping as a New Method in Geothermal Exploration: A Case Study from Central Nevada

Inga Moeck[1], Nick Hinz[2], James Faulds[2], John Bell[2], Annie Kell-Hills[3], and John Louie[3]

[1]International Centre for Geothermal Research, Potsdam, Germany
[2]Nevada Bureau of Mines and Geology, University of Nevada, Reno NV, USA
[3]Department of Geological Sciences and Engineering, University of Nevada, Reno NV, USA

Keywords

Geothermal exploration, 3D geological modelling, stress field determination, 3D fault stress modeling

ABSTRACT

Quantification of geological knowledge is critical in successful exploration and identification of geothermal reservoirs. Quantitative geology is expressed by 3D geological models, which are essential for an integrated approach in geothermal technology. Most 3D geological models are developed from subsurface data, such as seismic and well data. With this study, we present a 3D geological model developed primarily from surface data, specifically a detailed geological map. The study area is located along the east flank of the Wassuk Range and south end of Walker Lake basin in west-central Nevada.

The technique of 3D geological mapping involves digitizing of the geological map and selected cross sections, concatenating these scattered data with a digital elevation model by using a spline algorithm called the minimum tension technique. In the first step, a 3D fault model was developed, revealing the complex fault pattern of a graben structure in 3D space. Stratigraphic horizons were delineated after the fault blocks were defined. The final 3D structural model has been validated using 3D seismic data, which were integrated into part of the geological model. Conversely, the 3D geological model helped to validate interpretations of the 3D seismic data. Temperature, gravity, and well data were also integrated into the geological model to better understand the structural controls of this particular geothermal system.

Stress field determination was carried out by analysis of fault slip data. We apply the PTB method for stress field calculation and validate the derived stress field by fluctuation histograms and simulations of calculated versus measured shear stress vector.

With emphasis on fault behavior in the current stress field, we calculated shear and normal stress distribution along the mapped faults to discriminate between faults of high dilation and high slip tendency. Faults with high dilation tendency might primarily channel thermal fluids, thus providing favorable targets for geothermal exploitation. Based on this collective understanding, drill site selection and well path planning has been quantitatively defined.

Our case study shows how conventional geological maps can be employed to develop 3D structural geological models. We call this method 3D geological mapping, which can be used elsewhere provided geological maps are available.

1. Introduction

The model area lies within the Walker Lake domain of the central Walker Lane in the vicinity of Hawthorne, Nevada. The Walker Lane is a NW-striking dextral shear zone that accommodates ~20% o the Pacific-North American plate motion and stretches from southern California northward through western

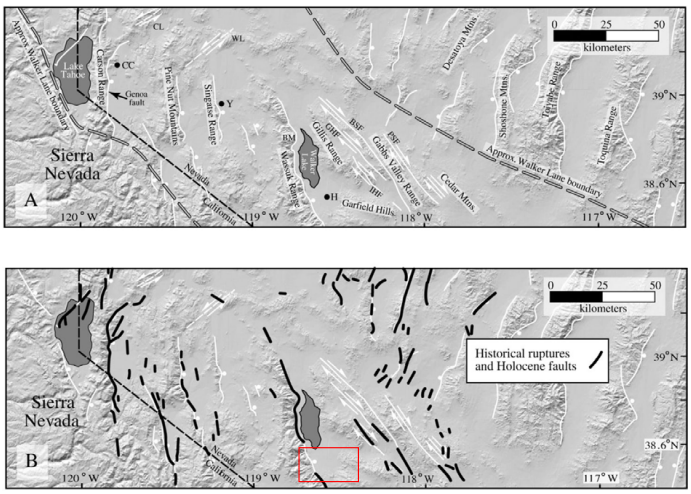

Figure 1. The Walker Lake domain and its structural pattern (modified from Surpless, 2008 and references therein). The red box indicates the study area. (A) Faults are displayed as white lines, with sense of slip is indicated on all major faults. White dots indicate dip direction. (B) Black faults are locations of historical ruptures (from Bell et al., 2004). See the seismically quiet segment of the Wassuk Range fault in the study area. Abbreviations: BM-Bald Mountain, BSF-Benton Spring fault, CC-Carson City, CL-Carson lineament, GHF-Gumdrop Hills fault, H-Hawthorne, IHF-Indian Hills fault, PSF-Petrified Springs fault, WL-Wabuska lineament, Y-Yerington

Nevada and northeastern California (Stewart, 1988; Faulds and Henry, 2008). Previous studies have shown that Miocene and younger normal and dextral faulting have deformed the Walker Lake region. In the western part of the Walker Lake domain, Miocene and younger deformation has been accommodated by E-W directed extension along major N-NNW-striking normal faults (Steward&Dohrenwend, 1984; Proffett and Dillies, 1984; Surpless, 1999, Schweickert et al., 2004). In the eastern part of the Walker Lake domain, dextral faults strike NNW-NW (Surpless, 2008) (Figure 1) subparallel to the overall trend of the Walker Lane.

The model area lies in the western portion of the Walker Lake domain, east of the Wassuk Range. It is locus of significant extensional deformation that migrated to the west from the Wassuk Range at ~15 Ma to the Serra Nevada frontal fault system at ~3 Ma (e.g. Schweickert et al., 2004). The motion along a series of N-NNW striking, east-dipping normal faults is primarily dip-slip (Surpless et al., 2002), resulting in a series of asymmetric half-grabens and mountain ranges across the area.

2. 3D Structural Geological Modeling

The preparation of the 3D geological modeling process required special attention to the generation of geologic cross sections. All faults and stratigraphic horizons require individual attribution to be clearly identified by the interpolation algorithm of the geological modeling procedure. Faults were therefore correlated between the cross-sections and the geologic map.

The geologic cross-sections with fully attributed faults and horizons were integrated into the 3D geological model. After extensive digitizing of cross sections and data editing, all data were imported in 3D space. The cross sections were merged with the geological map and digital elevation model to one coherent data set. The data set consists of fault data and horizon data (stratigraphy). The fault data set covers 55 different faults, and the horizon data set covers 5 geologic units (Table 1).

Table 1. Geologic units, displayed in the 3D structural geological model

Geologic unit	Description	Age
QTaa	Alluvial and lacustrine sediments	Quaternary
Tba	Basaltic andesitic lavas	Late Tertiary
Ts	Fluvial and lacustrine sediments	Late Tertiary
Ta	Andesite lavas	Late Tertiary
Basement	Metavolcanics, metasediments, granite	Mesozoic

All the input data are interpolated with the minimum tension technique, using the software earthVision. This technique is a spline algorithm based on distance weighted average - for interpolation of scattered input data. In a first step, a preliminary 3D fault model was developed. In a second step, the 3D fault model was refined and fault block geometries were defined by comparison with the geological map and seismic reflection data. The 3D fault model consists of 57 fault blocks. A binary fault hierarchy specifies the spatial relation of hanging walls and footwalls, whereas the fault planes are delineated by boundary polygons, defining the structural pattern. The calculated fault block geometries are used to integrate the horizon information. In a third step, the stratigraphy was integrated in the fault block so that a complete 3D structural geological model was developed, allowing for a complex collective interpretation.

3. Stress Field Determination

The stress field can be derived from fault slip data assuming a linear and direct relationship between strain and stress. Relating fault kinematics to stress states implies that all fault slip data were generated by the same deviatoric stress state. However, it is still under debate whether kinematic indicators from field based fault plane analysis can be used for stress field determination. One major challenge is the heterogeneity of data sets, caused by paleo stress fields or strain partitioning. In particular, strain partitioning along fault bends or relay ramps can evoke abnormal stress tensors in classical stress inversion from fault slip data (Angelier, 1994; Fodor, 2007). We present a methodology to calculate the stress tensor from field based data that incorporates possible local stress variations caused by strain partitioning and characteristic shear angles of different lithologies.

Our methodology involves the PTB method combined with a statistical analysis of shear stress vectors and stress ratios. The PTB method is a method that calculates the strain tensor from fault slip data. Assuming a linear relation of strain to stress, our methodology might deliver a reliable stress state when kinematically inconsistent structures are identified in the data set rather than in the field.

In particular, the PTB (P=Pressure T=Tension B=Intermediate) method is a kinematic analysis in brittle deformation that calculates the three theoretical principal strain axes for each individual fault-slip datum, i.e. a compressional axis P, a neutral axis B (which lies in the fault plane), and an extensional axis T (e.g. Sippel et al., 2009). Employing the Mohr-Coulomb failure criterion, the method incorporates a defined fracture angle between P and the slip surface. For this study, a fracture angle of 30° was applied. Assuming fault slip was induced by the same stress state, the orientation of each fault plane is dependent on the causative stress field. The application of PTB to the entire fault population of a particular location results in a comprehensive pattern of kinematic axes. Such a cumulative plot permits detection of kinematic consistencies as clusters of P, B, T axes in a heterogeneous data set.

The slip tendency method is also used in this study to calculate the state of stress of faults in the current stress field based on frictional constraints (Morris et al., 1996, Moeck et al., 2009). With this method, the ratio of shear to normal stress can be calculated for each fault or inferred faults. By calculating the normal stress, slip and dilation tendency can be determined. The slip tendency is expressed by

$$T_s=\tau/\sigma_{neff} \geq \mu_s \quad (1)$$

With Ts=slip tendency, τ =shear stress, σ_{neff} =effective normal stress, μ_s = friction coefficient. The dilation tendency is expressed by

$$\tau_d=(\sigma_1-\sigma_n) / (\sigma_1-\sigma_3) \quad (2)$$

If the slip tendency Ts equals or exceeds the frictional coefficient, the fault is likely to slip. Such a fault is referred to as critically stressed. Slip occurs when μ_s is between 0.6-0.8 (Byerlee, 1978). The dilation tendency is normalized to the normal stress σ_n and can have a maximum value of 1. Bi-modal dip refers to both possible dip directions, perpendicular to strike.

4. Results

The resulting 3D structural geological model shows the fault and horizon geometries of a NNW-trending graben structure (Figure 2). The release bend at the Wassuk Range front fault (red box in Figure 2, Figure 3) is an area of structural complexity presumably caused by secondary faults in a transtensional regime. The releasing bend has a dilational effect on the Wassuk Range front fault and on the geometry of the overall fault grain of this particular region (Figure 4).

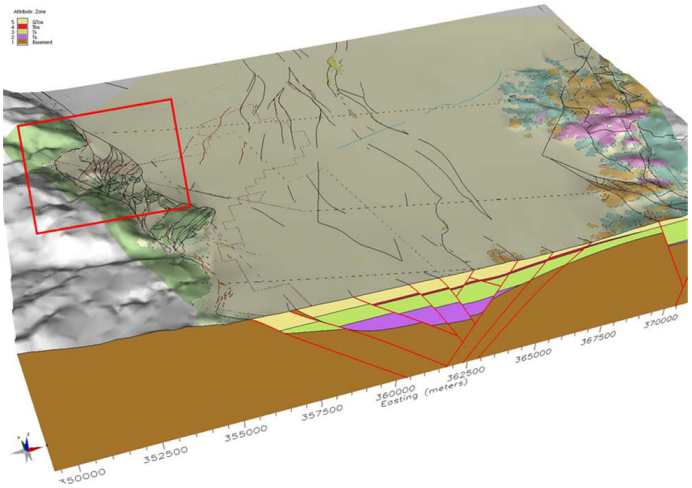

Figure 2. 3D geological model of the Hawthorne area. The red box surrounds the releasing bend at the Wassuk Range front fault. This area is shown in detail in figure 3.

Most of the faults yielding slip data strike NE-SW and indicate normal dip slip to oblique slip motion (Figure 5a). The stress field determination results in a normal faulting stress regime indicating extension in NW-SE direction (127°, Figure 5b). A fluctuation histogram shows the variation of calculated shear stress vector of the derived stress field to measured slip vectors (Figure 6). This variation shows basically the misfit of measured to calculated shear stress vectors and indicates different stress fields if two or more different peaks are present in the diagram (Meschede, 1994). The diagram in Figure 6b shows a half Gaussian distribution, indicating that half of the data set fits in the normal faulting stress regime and half of the data set has an error of more than 30%. The stress ratio, expressed by

$$R=(s2-s1)/(s3-s1), \quad (3)$$

indicates a transtensional stress regime with R=0.7(Figure 6a) (Delavaux & Sperner, 2003).

Applying the derived stress field for the slip and dilation tendency analysis, it is evident that fault planes with a NE-SW orientation have the highest slip and dilation tendency (Figure 7). It strongly depends, however, on the dip angle of faults as to whether they are likely to accommodate both dilation and shearing. Faults that dip 70°NW or SE (Figure 7) have the highest tendency to slip and to dilate.

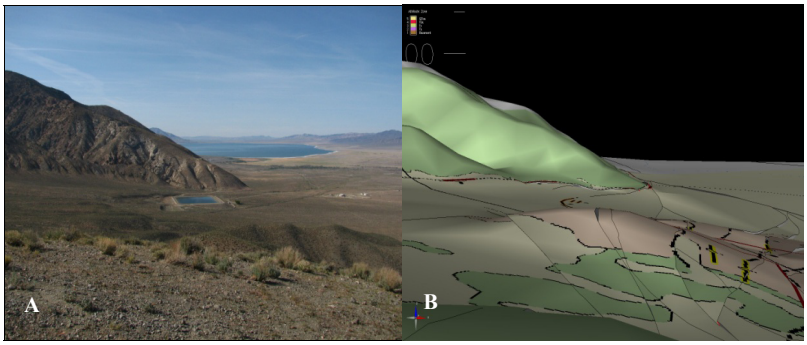

Figure 3. (A) Releasing bend at the Wassuk Range front fault, view from south to north (Walker Lake in the background). (B) Same spot of the photograph is visualized in the 3D geological model, covered by the geological map of the area (Hinz et al., this volume)

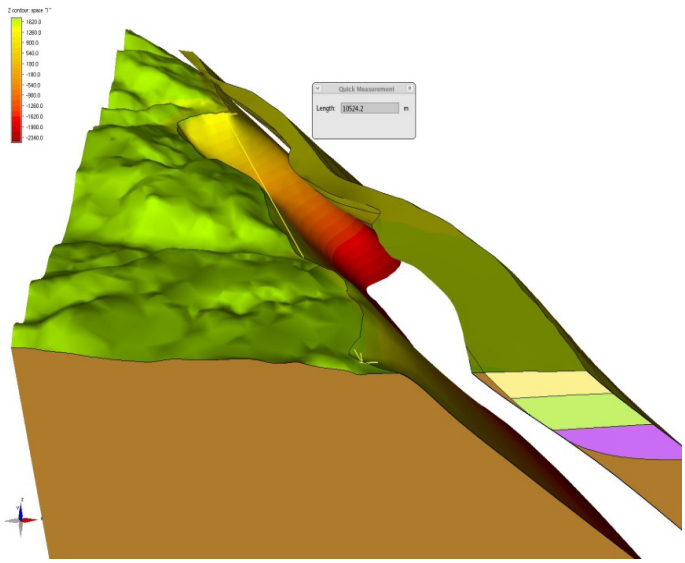

Figure 4. 3D perspective along the releasing bend at the Wassuk Range front fault. The release bend leads to a transtensional jog between two faults.

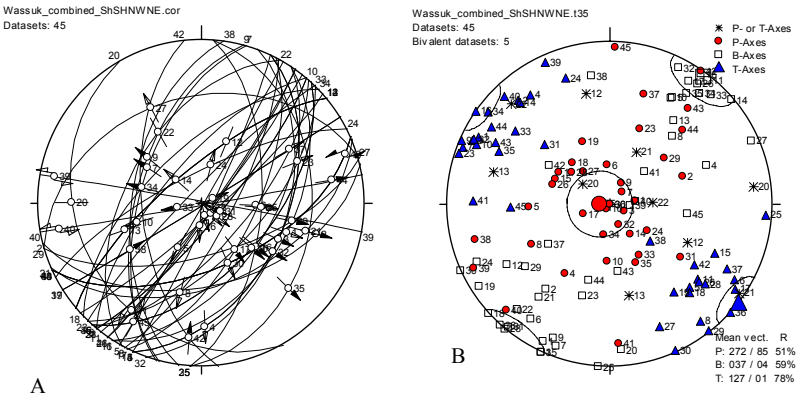

Figure 5. (A) Lower-hemisphere projection, Angelier-plot of the faults and slip vectors of faults, mapped by Hinz (Hinz et al., this volume). (B) PTB-plot of calculated strain axes, based on kinematic indicators of mapped faults.

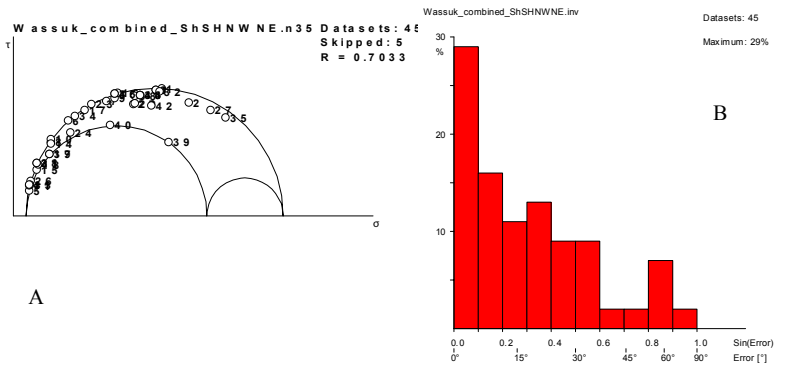

Figure 6. (A) Stress regime and stress ratio, expressed by the Mohr-Coulomb stress circle. (B) Fluctuation histogram of misfit angle between calculated and measured shear stress vector.

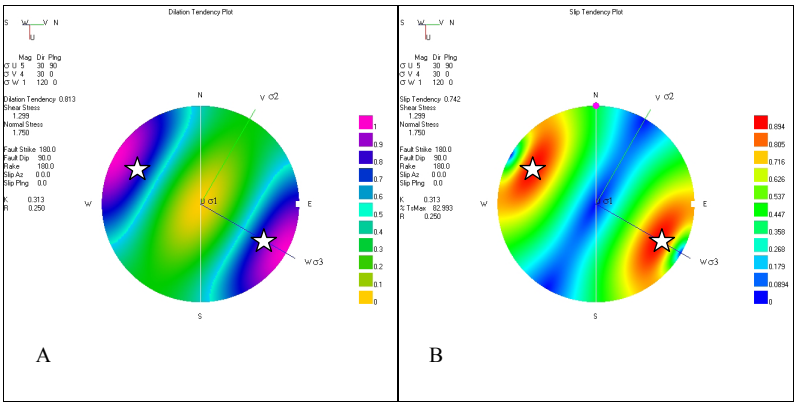

Figure 7. (A) Dilation tendency plot and (B) slip tendency plot, using the derived stress regime from this study. The star symbol indicates poles of planes, which are both highly dilational and prone to shearing, thus providing favorable structures for fluid flow.

5. Discussion and Conclusions

Stress field determination, based on kinematic indicators and field based fault plane analysis, yields a transtensional stress regime with a NW-trending extension direction. This agrees in general with syntheses of Surpless (2008), who describes both, extension and dextral shear for the central Walker Lane.

The PTB method and statistical analysis is an appropriate method to derive the stress field from fault slip data. In contrast to other direct inversion methods (e.g. Angelier, 1994, Marrett&Allmendinger, 1990), the PTB method allows the integration of shear angle, which is governed by mechanical properties of rock and varies in different lithologies. We used a shear angle of 35° for granitic rock (Pauzi et al., 2008). Slip and dilation tendency analysis indicate NW-striking, bi-modal 70° dipping fault planes as both highly dilational and shearing. This result explains the transtensional releasing bend along the Wassuk Range front fault. This region might be a favorable setting for geothermal fluid flow and should therefore be considered for further geothermal exploration.

The newly developed 3D structural geological model can be used for such an exploration campaign. We have demonstrated in our study that conventional geological maps provide sufficient data to develop a 3D geological model. Important for such an approach is the attributing of all elements that are contained by a geological map. With appropriate software and interpolation algorithms, data from geological maps can be combined with geophysical data that describe the structure of the subsurface. Some prior studies have shown that surface data from geological maps can be employed for 3D geological modeling (Dhont et al., 2005). We call this method 3D geological mapping, indicating the geological map as fundamental for 3D geological modeling. 3D geological mapping leads to a better understanding of 3D geometries of geological structures. Moreover, 3D geological maps can greatly enhance communication in projects in which various disciplines (geosciences and engineering) are working together for one aim as in geothermal field development. The quantification of geology by 3D geological models is crucial for multidisciplinary asset teams. Typically, geothermal exploration requires cost-efficient exploration methods. 3D geological modeling belongs to such a cost-efficient method, because geological maps are commonly available for many regions. Our approach can be adapted to other regions, provided high quality structural geological maps are available.

Acknowledgements

This project was funded by a grant from the U.S. Department of Navy. We thank Mike Lazaro and Andy Sabin of the Geothermal Program Office (GPO) of the Department of Navy and Greg Halsey of Epsilon Systems Inc. for support on this project. The 3D geological model was developed with earthVision (DGI). The stress field determination was carried out with TectonicsFP. The slip tendency analysis was carried out with the software 3DStress. We greatly thank Alan Morris for encouragement and helpful discussions.

References

Angelier, J., 1994. Fault slip analysis and paleostress field reconstruction, in Hancock, P.L., ed., Continental Deformation, Pergamon Press, Terrytown, New York, p. 53-100.

Byerlee, J.D., 1978. Friction of rocks. Pure Appl. Geophys. 116, 615-626.

Delavaux, D, Sperner, B. 2003. New aspects of tectonic stress inversion with reference to the TENSOR program. In: New insights into structural interpretation and modeling (D. A. Nieuwland, *ed.*). Geol. Soc. Spec. Pub., no. 212, 75-100.

Faulds, J.E., and Henry, C.D., 2008, Tectonic influences on the spatial and temporal evolution of the Walker Lane: An incipient transform fault along the evolving Pacific – North American plate boundary, *in* Spencer, J.E., and Titley, S.R., eds., Ores and orogenesis: Circum-Pacific tectonics, geologic evolution, and ore deposits: Arizona Geological Society Digest 22, p. 437-470.

Fodor, L.I., 2007. Segment linkage and the state of stress in transtensional transfer zones: field examples from the Pannonian Basin. Geological Society, London, Spec. Pub, v. 290, 417-431.

John, D.A.,1992. Stratigraphy, regional distribution, and reconnaissance geochemistry of Oligocene and Miocene volcanic rocks in the Paradise Range and northern Pactolus Hills, Nye County, Nevada. U.S.G.S. Bull. 1974. 67 pp.

Dhont, D., Luxey, P., Chorowicz, J., 2005. 3D modeling of geologic maps from surface data. AAPG Bull., 89/11, 1465-1474.

Marrett, R., Allmendinger, R.W., 1990, Kinematic analysis of fault-slip data: Journal of Structural Geology, v. 12, p. 973-986.

Meschede, M., 1994. Methoden der Strukturgeologie; ein Leitfaden zur Aufnahme und Auswertung strukturgeologischer Daten im Gelaende und im Labor. Enke, Stuttgart, Federal Republic of Germany, pp. 175.

Moeck, I., Kwiatek, G., Zimmermann, G., 2009, Slip tendency, fault reactivation potential and induced seismicity in a deep geothermal reservoir. J. Struct. Geol., 31, 1174-1182

Morris A., Ferril D.A., Henderson DB., 1996. Slip tendency analysis and fault reactivation. Geology 24(3), 275-278.

Pauzi, N.I.M., Omar, R.C., Roslan, R., 2008. Rock mass strength characteristics at Manjung area. ICCBT, E33, 403-414.

Proffett Jr. J.M., Dillies, J.H., 1984. Geologic map of the Yerington quadrangle, Nevada. NBMG, map 77.

Schweickert, R.A., Lahren, M.M., Smith, K.D., Howle, J.F., Ichinose, G., 2004. Transtensional deformation in the Lake Tahoe region, California and Nevada, USA. Tectonophysics 397, 303-323.

Sippel, J.; Scheck-Wenderoth, M.; Reicherter, K.; Mazur, S. (2009): Paleostress states at the south-western margin of the Central European Basin System — Application of fault-slip analysis to unravel a polyphase deformation pattern, Tectonophysics, 470, 1-2, 129-146

Stewart, J.H., Dohrenwend, J.C., 1984. Geologic map of the Yerington quadrangle, Nevada. USGS Open File Report 84-212.

Stewart, J.H., 1988, Tectonics of the Walker Lane belt, western Great Basin: Mesozoic and Cenozoic deformation in a zone of shear, *in* Ernst, W.G., ed., The geotectonic development of California: Englewood Cliffs, New Jersey, Prentice-Hall, p. 7186.

Stockli, D.F., Surpless, B.E., Dumitru, T.A., Farley, K.A., 2002. Thermochronological constraints on the timing and magnitude of Miocene and Pliocene extension in the central Wassuk Range, western Nevada. Tectonics 21(4), 1028-1047.

Surpless, B.E., 1999. A structural, magmatic, and thermochronological study of the central Wassuk Range, western Nevada. Tectonics 21(4), doi:10.1029/2000TC001257

Surpless, B.E., Stockli, D.F., Dumitru, T.A., Miller, E.L., 2002. Two-phase westward encroachment of Basin and Range extension into the northern Sierra Nevada. Tectonics 21(4), doi: 10.1029/2000TC001257.

Surpless, B., 2008. Modern strain localization in the central Walker Lane, western United States: Implications for the evolution of intraplate deformation in transtensional settings. Tectonophysics, 457, 239-253.